
Repetitive Reprediction Deep Decipher for Semi-Supervised Learning

Guo-Hua Wang, Jianxin Wu

National Key Laboratory for Novel Software Technology
Nanjing University
Nanjing, China

wangguohua@lamda.nju.edu.cn, wujx2001@nju.edu.cn

Abstract

Most recent semi-supervised deep learning (deep SSL) methods used a similar paradigm: use network predictions to update pseudo-labels and use pseudo-labels to update network parameters iteratively. However, they lack theoretical support and can not explain why predictions are good candidates for pseudo-labels. In this paper, we propose a principled end-to-end framework named deep decipher (D2) for SSL. With the D2 framework, we prove that pseudo-labels are related to network predictions by an exponential link function, which gives a theoretical support for using predictions as pseudo-labels. Furthermore, we demonstrate that updating pseudo-labels by network predictions will make them uncertain. To mitigate this problem, we propose a training strategy called repetitive reprediction (R2). Finally, the proposed R2-D2 method is tested on the large-scale ImageNet dataset and outperforms state-of-the-art methods by 5%.

1 Introduction

Deep learning has achieved state-of-the-art results on many visual recognition tasks. However, training these models often needs large-scale datasets such as ImageNet [17]. Nowadays, it is easy to collect images by search engines, but image annotation is expensive and time-consuming. Semi-supervised learning (SSL) is a paradigm to learn a model with a few labeled data and massive amounts of unlabeled data. With the help of unlabeled data, the model performance may be improved.

With a supervised loss, unlabeled data can be used in training by assigning pseudo-labels to them. Many state-of-the-art methods on semi-supervised deep learning used pseudo-labels implicitly. Temporal Ensembling [7] used the moving average of network predictions as pseudo-labels. Mean Teacher [20] and Deep Co-training [15] employed another network to generate pseudo-labels. However, they produced or updated pseudo-labels in ad-hoc manners. Although these methods worked well in practice, there are few theories to support them. A mystery in deep SSL arises: why can predictions work well as pseudo-labels?

In this paper, we propose an end-to-end framework called deep decipher (D2). Inspired by [22], we treat pseudo-labels as variables and update them by back-propagation, which is also learned from data. And the pseudo-label is a probability distribution among all possible classes. With deep decipher, we prove that there exists an exponential relationship between pseudo-labels and network predictions, leading to a theoretical support for using network predictions as pseudo-labels. Then, we further analyze the D2 framework and prove that pseudo-labels will become flat (i.e., their entropy is high) during training and there is an equality constraint bias in it. To mitigate these problems, we propose a simple but effective strategy, repetitive reprediction (R2). The improved D2 framework is named R2-D2 and obtained state-of-the-art results on several SSL problems.

Our contributions are as follows.

- We propose D2, a deep learning framework that deciphers the relationship between predictions and pseudo-labels. D2 updates pseudo-labels by back-propagation. To the best of our knowledge, D2 is the first deep SSL method that learns pseudo-labels from data end-to-end.
- Within D2, we prove that pseudo-labels are exponentially transformed from the predictions. Hence, it is reasonable for previous works to use network predictions as pseudo-labels. Meanwhile, many SSL methods can be considered as special cases of D2 in certain aspects.
- To further boost D2’s performance, we find some shortcomings of D2. In particular, we prove that pseudo-labels will become flat during the optimization. To mitigate this problem, we propose a simple but effective remedy, R2. We tested the R2-D2 method on ImageNet [17] and it outperforms state-of-the-arts by a large margin. On small-scale datasets like CIFAR-10 [6], R2-D2 also produces state-of-the-art results.

2 Related Works

We first briefly review deep SSL methods and the related works that inspired this paper.

[9] is an early work on training deep SSL models by pseudo-labels, which picks the class with the maximum predicted probability as pseudo-labels for unlabeled images and tested only on a small-scale dataset MNIST [8]. Label propagation [23] can be seen as a form of pseudo-labels. Based on some metric, label propagation pushes the label information of each sample to the near samples. [21] applies label propagation to deep learning models. Iscen et al. [5] use the manifold assumption to generate pseudo-labels for unlabeled data. However, their method is complicated and relied on other SSL methods to produce state-of-the-art results.

Several recent state-of-the-art deep SSL methods can be considered as using pseudo-labels implicitly. Temporal ensembling [7] proposes making the current prediction and the pseudo-labels consistent, where the pseudo-labels take into account the network predictions over multiple previous training epochs. Extending this idea, Mean Teacher [20] employs a secondary model, which uses the exponential moving average weights to generate pseudo-labels. Virtual Adversarial Training [12] uses network predictions as pseudo-labels, then they want the network predictions under adversarial perturbation to be consistent with pseudo-labels. Deep Co-Training [15] employs many networks and uses one network to generate pseudo-labels for training other networks.

We notice that they all use the network predictions as pseudo-labels but a theory explaining its rationale is missing. With our D2 framework, we demonstrate that pseudo-labels will indeed be related to network predictions. That gives a theoretical support to using network predictions as pseudo-labels. Moreover, pseudo-labels of previous works were designed manually and ad-hoc, but our pseudo-labels are updated by training the end-to-end framework. Many previous SSL methods can also be considered as special cases of the D2 framework in certain aspects.

There are some previous works in other fields that inspired this work. Deep label distribution learning [2] inspired us to use label distributions to encode the pseudo-labels. [19] studies the label noise problem. They find it is possible to update the noisy label to make them more precise during the training. PENCIL [22] proposes an end-to-end framework to train the network and optimize the noisy labels together. Our method is inspired by PENCIL [22]. In addition, inspired by [10], we analyze our algorithm from the gradient perspective.

3 The R2-D2 Method

We define the notations first. Column vectors and matrices are denoted in bold (e.g., \mathbf{x} , \mathbf{X}). When $\mathbf{x} \in \mathbb{R}^d$, x_i is the i -th element of vector \mathbf{x} , $i \in [d]$, where $[d] := \{1, 2, \dots, d\}$. \mathbf{w}_i denote the i -th column of matrix $\mathbf{W} \in \mathbb{R}^{d \times l}$, $i \in [l]$. And, we assume the dataset has N classes.

3.1 Deep decipher

Figure 1 shows the D2 pipeline, which is inspired by [22]. Given an input image \mathbf{x} , D2 can employ any backbone network to generate feature $\mathbf{f} \in \mathbb{R}^D$. Then, the linear activation $\hat{\mathbf{y}} \in \mathbb{R}^N$ is computed as $\hat{\mathbf{y}} = \mathbf{W}^T \mathbf{f}$, where $\mathbf{W} \in \mathbb{R}^{D \times N}$ are weights of the FC layer and we omit the bias term for

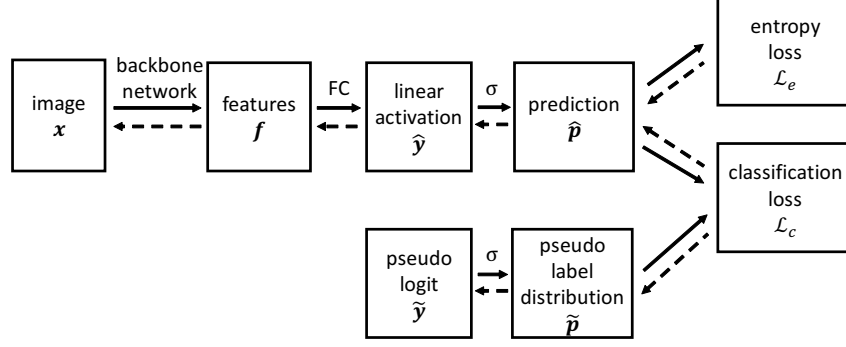


Figure 1: The pipeline of D2. Solid lines and dashed lines represent the forward and back-propagation processes, respectively.

simplicity. The softmax function is denoted as $\sigma(\mathbf{x}) : \mathbb{R}^N \rightarrow \mathbb{R}^N$ and $\sigma(\mathbf{x})_i = \frac{\exp(x_i)}{\sum_{j=1}^N \exp(x_j)}$. Then, the prediction $\hat{\mathbf{p}}$ is calculated as $\hat{\mathbf{p}} = \sigma(\hat{\mathbf{y}})$, hence

$$\hat{p}_n = \sigma(\hat{\mathbf{y}})_n = \sigma(\mathbf{W}^\top \mathbf{f})_n = \frac{\exp(\mathbf{w}_n^\top \mathbf{f})}{\sum_{i=1}^N \exp(\mathbf{w}_i^\top \mathbf{f})}. \quad (1)$$

We define $\tilde{\mathbf{y}}$ as the pseudo logit which is an unconstrained variable and *can* be updated by back-propagation. Then, the pseudo label is calculated as $\tilde{\mathbf{p}} = \sigma(\tilde{\mathbf{y}})$ and it is a probability distribution.

In the training, the D2 framework is initialized as follows. Firstly, we train the backbone network using only labeled examples, and use this trained network as the backbone network and FC in Figure 1. For labeled examples, $\tilde{\mathbf{y}}$ is initialized by $K\mathbf{y}$, in which $K = 10$ and \mathbf{y} is the groundtruth label in the one-hot encoding. Note that $\tilde{\mathbf{y}}$ of labeled examples will *not* be updated during D2 training. For unlabeled examples, we use the trained network to predict $\hat{\mathbf{y}}$. That means we use the FC layer activation $\hat{\mathbf{y}}$ as the initial value of $\tilde{\mathbf{y}}$. The process of initializing pseudo-labels is called predicting pseudo-labels in this paper. In the testing, we use the backbone network with FC layer to make predictions and the branch of pseudo-labels is removed.

Our loss function consists of \mathcal{L}_c and \mathcal{L}_e . \mathcal{L}_c is the classification loss and defined as $KL(\hat{\mathbf{p}} \parallel \tilde{\mathbf{p}})$ as in [22], which is different from the classic KL-loss $KL(\hat{\mathbf{p}} \parallel \hat{\mathbf{p}})$. \mathcal{L}_c is used to make the network predictions match the pseudo-labels. \mathcal{L}_e is the entropy loss, defined as $-\sum_{j=1}^N \hat{p}_j \log(\hat{p}_j)$. Minimizing the entropy of the network prediction can encourage the network to peak at only one category. So our loss function is defined as

$$\mathcal{L} = \alpha \mathcal{L}_c + \beta \mathcal{L}_e = \alpha \sum_{j=1}^N \hat{p}_j [\log(\hat{p}_j) - \log(\tilde{p}_j)] - \beta \sum_{j=1}^N \hat{p}_j \log(\hat{p}_j), \quad (2)$$

where α and β are two hyperparameters. Although here are two hyperparameters, we always set $\alpha = 0.1$ and $\beta = 0.03$ in all our experiments.

Then, we show that we can decipher the relationship between pseudo-labels and network predictions in D2, as shown by Theorem 1.

Theorem 1 Suppose D2 is trained by SGD with the loss function $\mathcal{L} = \alpha \mathcal{L}_c + \beta \mathcal{L}_e$. Let $\hat{\mathbf{p}}$ denote the prediction by the network for one example and \hat{p}_n is the largest value in $\hat{\mathbf{p}}$. After the optimization algorithm converges, we have $\tilde{p}_n \rightarrow \exp(-\frac{\mathcal{L}}{\alpha}) (\hat{p}_n)^{1-\frac{\beta}{\alpha}}$.

The complete proof is given in Appendix A.1. Theorem 1 tells us \tilde{p}_n converges to $\exp(-\frac{\mathcal{L}}{\alpha}) (\hat{p}_n)^{1-\frac{\beta}{\alpha}}$ during the optimization. And at last, we expect that $\tilde{p}_n = \exp(-\frac{\mathcal{L}}{\alpha}) (\hat{p}_n)^{1-\frac{\beta}{\alpha}}$, in which n is the class predicted by the network. Appendix Figure 3 shows the experiment results for this theorem, which holds well in practice.

In other words, we decipher that there is an exponential link between pseudo-labels and predictions. From $\tilde{p}_n \rightarrow \exp(-\frac{\beta}{\alpha}) (\hat{p}_n)^{1-\frac{\beta}{\alpha}}$, we notice that \tilde{p}_n is approximately proportional to $\hat{p}_n^{1-\frac{\beta}{\alpha}}$. That gives a theoretical support to use network predictions as pseudo-labels. And, it is required that $1 - \frac{\beta}{\alpha} > 0$ to make pseudo-labels and network predictions consistent. We must set $\alpha > \beta$. In our experiments, if we set $\alpha < \beta$, the training will indeed fail miserably.

Next, we analyze how $\tilde{\mathbf{y}}$ is updated in D2. With the loss function \mathcal{L} , the gradients of \mathcal{L} with respect to \tilde{y}_n is

$$\frac{\partial \mathcal{L}}{\partial \tilde{y}_n} = -\alpha \sigma(\hat{\mathbf{y}})_n + \alpha \sigma(\tilde{\mathbf{y}})_n. \quad (3)$$

The complete derivation is given in Appendix A.3. By back-propagation, the pseudo logit $\tilde{\mathbf{y}}$ is updated by

$$\tilde{\mathbf{y}} \leftarrow \tilde{\mathbf{y}} - \lambda \frac{\partial \mathcal{L}}{\partial \tilde{\mathbf{y}}} = \tilde{\mathbf{y}} - \lambda \alpha \sigma(\tilde{\mathbf{y}}) + \lambda \alpha \sigma(\hat{\mathbf{y}}), \quad (4)$$

where λ is the learning rate for updating $\tilde{\mathbf{y}}$. The reason we use one more hyperparameter λ rather than the overall learning rate is that $\frac{\partial \mathcal{L}}{\partial \tilde{\mathbf{y}}} = -\alpha \sigma(\hat{\mathbf{y}}) + \alpha \sigma(\tilde{\mathbf{y}})$ is smaller than $\tilde{\mathbf{y}}$ (in part due to the sigmoid transform) and the overall learning rate is too small to update the pseudo logit (cf. Appendix Figure 8). We set $\lambda = 4000$ in all our experiments.

The updating formulas in many previous works can be considered as special cases of D2. In Temporal Ensembling [7], the pseudo-labels $\tilde{\mathbf{p}}$ is a moving average of the network predictions $\hat{\mathbf{p}}$ during training. The updating formula is $\mathbf{P} \leftarrow \alpha \mathbf{P} + (1 - \alpha) \hat{\mathbf{p}}$. To correct for the startup bias, the $\tilde{\mathbf{p}}$ is needed to be divided by factor $(1 - \alpha^t)$, where t is the number of epochs. So the updating formula of $\tilde{\mathbf{p}}$ is $\tilde{\mathbf{p}} \leftarrow \mathbf{P} / (1 - \alpha^t)$. In Mean Teacher [20], the $\tilde{\mathbf{p}}$ is the prediction of a teacher model which uses the exponential moving average weights of the student model. Tanaka et al. [19] proposed using the running average of the network predictions to estimate the groundtruth of the noisy label. However, their updating formula were designed manually and ad-hoc. In contrast, our updating formula comes from the end-to-end framework, which is more principled and natural.

3.2 A toy example

Now, we use a toy example to explain how the D2 framework works intuitively. Inspired by [10], we use the LeNet [8] as backbone structure and add two FC layers, in which the first FC layer learns a 2-D feature and the second FC layer projects the feature onto the class space. The network was trained on MNIST [8]. Note that MNIST [8] has 60000 images for training. We only used 1000 images as labeled images to train the network. Figure 2a depicts the 2-D feature distribution of these 1000 images. We observe that features belonging to the same class will cluster together. Figure 2b shows the feature distribution of both these 1000 labeled and other 49000 unlabeled images. Although the network did not train on the unlabeled images, features belonging to the same class are still roughly clustered.

Pseudo-labels in our D2 framework are probability distributions and initialized by network predictions. As Figure 2b shows, features near the cluster center will have confident pseudo-labels and can be learned safely. However, features at the boundaries between clusters will have a pseudo-label whose corresponding distribution among different classes is flat rather than sharp. By training D2, the network will learn confident pseudo-labels first. Then it is expected that unconfident pseudo-labels will become more and more precise and confident by optimization. At last, each cluster will become more compact and the boundaries between different classes' features will become clear. Figure 2d depicts the feature distribution of all images after D2 training. Because the same class features of unlabeled images get closer, the same class features of labeled images will also get closer (cf. Figure 2c). That is how unlabeled images help training in our D2 framework.

3.3 Repetitive reprediction

Although D2 has worked well in practice (cf. Table 1 line a), there are still some shortcomings in it. We will discuss two major ones. To mitigate these problems and further boost the performance, we propose a simple but effective strategy, repetitive reprediction (R2), to improve the D2 framework.

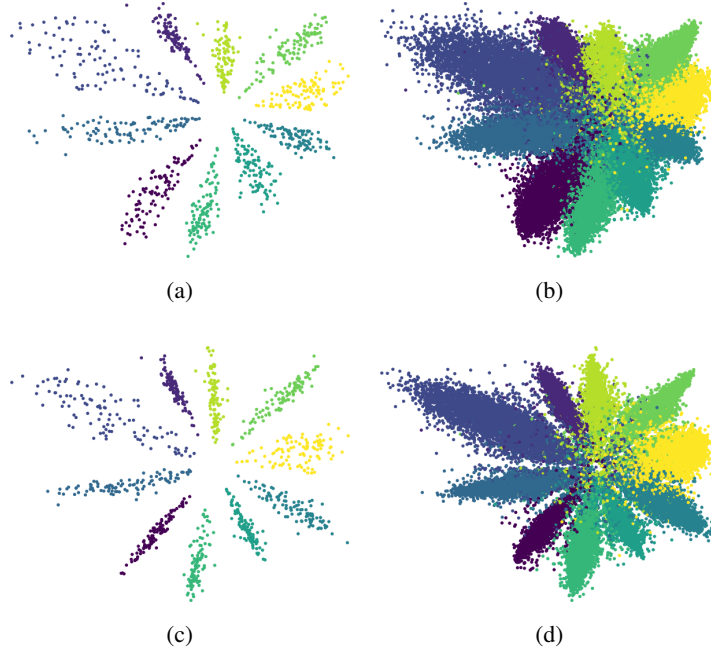


Figure 2: Feature distribution on MNIST [8]. First, LeNet was trained by labeled data. (a) shows the the feature distribution of labeled images. Points with the same color belong to the same class. (b) shows the feature distribution of both labeled and unlabeled images. Then, we used LeNet as the backbone network and trained the D2 framework. After training, (c) and (d) show the feature distribution of labeled images and all images, respectively.

First, we expect pseudo-labels can become more confident along with D2’s learning process. Unfortunately, we observed that more and more pseudo-labels become flat during training (cf. Appendix Figure 5). Below, we prove Theorem 2 to explain why this adverse effect happens.

Theorem 2 *Suppose D2 is trained by SGD with the loss function $\mathcal{L} = \alpha\mathcal{L}_c + \beta\mathcal{L}_e$. If $\tilde{p}_n = \exp(-\frac{\mathcal{L}}{\alpha})(\hat{p}_n)^{1-\frac{\beta}{\alpha}}$, we must have $\tilde{p}_n \leq \hat{p}_n$.*

The complete proof is given in Appendix A.2. From Theorem 1, we get $\tilde{p}_n \rightarrow \exp(-\frac{\mathcal{L}}{\alpha})(\hat{p}_n)^{1-\frac{\beta}{\alpha}}$, where $\hat{\mathbf{p}}$ gets the largest value at \hat{p}_n . And Theorem 2 tells us if $\tilde{p}_n = \exp(-\frac{\mathcal{L}}{\alpha})(\hat{p}_n)^{1-\frac{\beta}{\alpha}}$ then \tilde{p}_n will be smaller than \hat{p}_n . Because $\tilde{\mathbf{p}}$ and $\hat{\mathbf{p}}$ are probability distributions, if $\tilde{\mathbf{p}}$ and $\hat{\mathbf{p}}$ get their largest value at n , $\tilde{\mathbf{p}}$ is more flat than $\hat{\mathbf{p}}$ when $\tilde{p}_n \leq \hat{p}_n$. That is, along with the training of D2, there is a tendency that pseudo-labels will be more flat than the network predictions.

Second, we find an unsolicited bias in the D2 framework. From the updating formula, we can get

$$\sum_{i=1}^N \tilde{y}_i \leftarrow \sum_{i=1}^N \tilde{y}_i - \lambda\alpha \sum_{i=1}^N \sigma(\tilde{\mathbf{y}})_i + \lambda\alpha \sum_{i=1}^N \sigma(\hat{\mathbf{y}})_i = \sum_{i=1}^N \tilde{y}_i - \lambda\alpha + \lambda\alpha = \sum_{i=1}^N \tilde{y}_i. \quad (5)$$

That is, $\sum_{i=1}^N \tilde{y}_i$ will *not* change after initialization. Although we define $\tilde{\mathbf{y}}$ as the variable which is not constrained, the softmax function and SGD set an equality constraint for it. On the other hand, in practice, $\sum_{i=1}^N \hat{y}_i$ become more and more concentrated (cf. Appendix Figure 7). We will use an ablation study to demonstrate this bias is harmful.

We propose a repetitive reprediction (R2) strategy to overcome these difficulties, which repeatedly perform repredictions (i.e., using the prediction $\tilde{\mathbf{y}}$ to re-initialize the pseudo-labels $\tilde{\mathbf{y}}$ several times) during training D2. The benefits of R2 are two-fold. First, we want to make pseudo-labels confident. According to our analysis, the network predictions are sharper than pseudo-labels when the algorithm

converges. So repredicting pseudo-labels can make them sharper. Second, $\sum_{i=1}^N \tilde{y}_i$ will not change during D2 training. Reprediction can reduce the impact of this bias. Furthermore, the validation accuracy often increase during training. A repeated reprediction can make pseudo-labels more accurate than that of last reprediction.

Apart from the repredictions, we also reduce the learning rate to boost the performance. If the D2 framework is trained by a fixed learning rate (as in [22]), the loss \mathcal{L} did not descend in experiments (cf. Appendix Figure 9). Reducing the learning rate can make the loss descend (cf. Appendix Figure 10). We can get some benefits from a lower loss. On one hand, \mathcal{L}_c is the KL divergence between pseudo-labels and the network predictions. Minimizing this term makes pseudo-labels as sharp as the network predictions. On the other hand, minimizing \mathcal{L}_e can decrease the entropy of network predictions. So when it comes to next reprediction, pseudo-labels will be more confident according to sharper predictions.

Finally, repredicting pseudo-labels frequently is harmful for performance. By using the R2 strategy every epoch, the network predictions and pseudo-labels are always the same and D2 can not optimize pseudo-labels anymore. In CIFAR-10 experiments, we repredict pseudo-labels every 75 epochs and reduce the learning rate after each reprediction. Appendix Figure 6 shows that using the R2 strategy can make pseudo-labels more confident at the end of training.

3.4 The overall R2-D2 algorithm

Now we propose the overall R2-D2 algorithm. The training can be divided into three stages. In the first stage, we only use labeled images to train the backbone network with cross entropy loss as in common network training. In the second stage, we use the backbone network trained in the first stage to predict pseudo-labels for unlabeled images. Then we use D2 to train the network and optimize pseudo-labels together. It is expected that this stage can boost the network performance and make pseudo-labels more precise. But according to our analysis, it is not enough to train D2 by only one stage. With the R2 strategy, D2 will be repredicted and trained for several times. In the third stage, the backbone network is finetuned by all images whose labels come from the second stage. For unlabeled images, we pick the class which has the maximum value in pseudo-labels and use the cross entropy loss to train the network. And pseudo-labels are not updated anymore. For labeled images, we use their groundtruth labels.

4 Experiments

In this section, we use three datasets to evaluate our algorithm: ImageNet [17], CIFAR-10 [6], SVHN [13]. We first use an ablation study to investigate the impact of the R2 strategy. We then report the results on these datasets to compare with state-of-the-arts. All experiments were implemented using the PyTorch framework and run on a computer with TITAN Xp GPU.

4.1 Implementation details

Note that we trained the network using stochastic gradient descent with Nesterov momentum 0.9 in all experiments. We set $\alpha = 0.1$, $\beta = 0.03$ and $\lambda = 4000$ on *all* datasets, which shows the robustness of our method to these hyperparameters. Other hyperparameters (e.g., batch size, learning rate, and weight decay) were set according different datasets.

ImageNet is a large-scale dataset with natural color images from 1000 categories. Each category typically has 1300 images for training and 50 for evaluation. Following the prior work [15, 18, 14, 20], we uniformly choose 10% data from training images as labeled data. That means there are 128 labeled data for each category. The rest of training images are considered as unlabeled data. We test our model on the validation set. The backbone network was ResNet-18 [4]. More details can be found in Appendix B.1.

CIFAR-10 contains 32×32 natural images from 10 categories. Following [7, 12, 20, 15, 16], we used 4000 images (400 per class) from 50000 training images as labeled data and the rest images as unlabeled data. We report the error rates on the full 10000 testing images. The backbone network was Shake-Shake [3]. More details can be found in Appendix B.2.

Table 1: Ablation studies when using different strategies to train our end-to-end framework.

	The 2nd stage	Repeat the 2nd stage	Reprediction	Reducing LR	Error rates (%)
a	✓				6.71
b	✓	✓			6.37
c	✓	✓	✓		6.23
d	✓	✓		✓	5.94
e	✓	✓	✓	✓	5.78

Table 2: Error rates (%) on the validation set of ImageNet benchmark with 10% images labeled. “-” means that the original papers did not report the corresponding error rates.

	Method	Backbone	#Param	Top-1	Top-5
Supervised	100% Supervised [15]	ResNet-18	11.6M	30.43	10.76
	10% Supervised [15]	ResNet-18	11.6M	52.23	27.54
Semi-supervised	Stochastic Transformations [18]	AlexNet	61.1M	-	39.84
	VAE [14] with 10% Supervised	Customized	30.6M	51.59	35.24
	Mean Teacher [20]	ResNet-18	11.6M	49.07	23.59
	Dual-View Deep Co-Training [15]	ResNet-18	11.6M	46.50	22.73
	R2-D2	ResNet-18	11.6M	41.55	19.52

SVHN dataset consists of 32×32 house number images belonging to 10 classes. The category of each image is the centermost digit. There are 73257 training images and 26032 testing images in SVHN. Following [7, 20, 12, 15], we use 1000 images (100 per class) as labeled data and the rest 72257 training images as unlabeled data. The backbone network was ConvLarge [7]. More details can be found in Appendix B.3.

4.2 Ablation study

Now we validate our framework by an ablation study on CIFAR-10 with Shake-Shake backbone and 4000 labeled images. All experiments used the same data splits and ran once. And they all used the first stage to initialize D2 and the third stage to finetune the network. Table 1 presents the results and the error rates are produced by the last epoch of the third stage. Different lines denote using different strategies to train D2 in the second stage. First, without R2 (line a), the error rate of a basic D2 learning is 6.71%, which is already competitive with state-of-the-arts. Next, we repeated the second stage without reprediction or reducing learning rate (line b). That means the network is trained by the first stage, the second stage, repeat the second stage, and the third stage. This network achieved a 6.37% error rate, which demonstrates training D2 for more epochs can boost performance and the network can not overfit easily. Repeating the second stage with reprediction (line c) could make the error rate even lower, to 6.23%. But without reducing the learning rate, \mathcal{L} did not decrease (cf. Appendix Figure 11c). On the other hand, repeating the second stage and reducing the learning rate (line d) can get better results (5.94%). However, only reducing the learning rate can not remove the impact of the equality constraint bias. At last, applying both strategies (line e) improved the results by a large margin to 5.78%.

4.3 Results on ImageNet

Table 2 shows our results on ImageNet with 10% labeled samples. The setup followed that in [15]. The image size in training and testing is 224×224 . For the fairness of comparisons, the error rate is from single model without ensembling. We use the result of the last epoch. Our experiment is repeated three times with different random subsets of labeled training samples. The Top-1 error rates are 41.64, 41.35, and 41.65, respectively. The Top-5 error rates are 19.53, 19.60, and 19.44, respectively. R2-D2 achieves significantly lower error rates than Stochastic Transformations [18] and VAE [14], although they used the larger input size 256×256 . With the same backbone and input size, R2-D2 obtains roughly 5% lower Top-1 error rate than that of DCT [15] and 7.5% lower Top-1 error rate than that of Mean Teacher [20]. R2-D2 outperforms the previous state-of-the-arts by a large margin. The performances of Mean Teacher [20] with ResNet-18 [4] is quoted from [15].

Table 3: Error rates (%) on CIFAR-10 benchmark with 4000 images labeled.

	Method	Backbone	Error rates (%)
Supervised	100% Supervised [3]	Shake-Shake	2.86
	Using 4000 labeled images only	Shake-Shake	14.90 ± 0.28
Semi-supervised	Mean Teacher [20]	ConvLarge	12.31 ± 0.28
	Temporal Ensembling [7]	ConvLarge	12.16 ± 0.24
	VAT+EntMin [12]	ConvLarge	10.55 ± 0.05
	Deep Co-Training with 8 Views [15]	ConvLarge	8.35 ± 0.06
	Mean Teacher [20]	Shake-Shake	6.28 ± 0.15
	HybridNet [16]	Shake-Shake	6.09
	R2-D2	Shake-Shake	5.72 ± 0.06

Table 4: Error rates (%) on SVHN benchmark with 1000 images labeled.

	Method	Backbone	Error rates (%)
Supervised	100% Supervised [7]	ConvLarge	2.88 ± 0.03
	Using 1000 labeled images only	ConvLarge	11.27 ± 0.85
Semi-supervised	Temporal Ensembling [7]	ConvLarge	4.42 ± 0.16
	Mean Teacher [20]	ConvLarge	3.95 ± 0.19
	VAT+EntMin [12]	ConvLarge	3.86 ± 0.11
	Deep Co-Training with 8 Views [15]	ConvLarge	3.29 ± 0.03
	R2-D2	ConvLarge	3.64 ± 0.20

4.4 Results on CIFAR-10

We evaluated the performance of R2-D2 on CIFAR-10 with 4000 labeled samples. Table 3 presents the results. Following [20, 16], we used the Shake-Shake network [3] as the backbone network. Our experiment was repeated five times with different random subsets of labeled training samples. We used the test error rates of the last epoch. After the first stage, the backbone network produced the error rates 14.90%, which is our baseline using 4000 labeled samples. Compared with existing deep SSL methods, R2-D2 achieves lower error rate and produces state-of-the-art results.

4.5 Results on SVHN

We tested R2-D2 on SVHN with 1000 labeled samples. The results are shown in Table 4. Following previous works [7, 20, 12, 15], we used the ConvLarge network as the backbone network. The result we report is average error rate of the last epoch over five random data splits. On this task, the gap between 100% supervised and many SSL methods (e.g., VAT+EntMin [12], Deep Co-Training [15], and R2-D2) is less than 1%. Only Deep Co-Training with 8 Views [15] slightly outperforms R2-D2. Compared with other methods (e.g., Temporal Ensembling [7], Mean Teacher [20], and VAT [12]), R2-D2 produces lower error rate. Note that on the large-scale ImageNet [17], R2-D2 significantly outperformed Deep Co-Training.

5 Conclusion

In this paper, we proposed R2-D2, a method for semi-supervised deep learning. D2 uses label probability distributions as pseudo-labels for unlabeled images and optimizes them during training. Unlike previous SSL methods, D2 is an end-to-end framework which is independent of the backbone network and can be trained by back-propagation. Based on D2, we give a theoretical support for using network predictions as pseudo-labels. However, pseudo-labels will become flat during training. We analyzed this problem both theoretically and experimentally, and proposed the R2 remedy for it. At last, we tested R2-D2 on different datasets. On large-scale dataset ImageNet, R2-D2 achieved about 5% lower error rates than that of previous state-of-the-art. In the future, we will explore the combination of unsupervised feature learning and semi-supervised learning.

References

- [1] Terrance DeVries and Graham W Taylor. Improved regularization of convolutional neural networks with cutout. *arXiv preprint arXiv:1708.04552*, 2017.
- [2] Bin-Bin Gao, Chao Xing, Chen-Wei Xie, Jianxin Wu, and Xin Geng. Deep label distribution learning with label ambiguity. *IEEE Transactions on Image Processing*, 26(6):2825–2838, 2017.
- [3] Xavier Gastaldi. Shake-shake regularization. *arXiv preprint arXiv:1705.07485*, 2017.
- [4] Kaiming He, Xiangyu Zhang, Shaoqing Ren, and Jian Sun. Deep residual learning for image recognition. In *The IEEE Conference on Computer Vision and Pattern Recognition (CVPR)*, pages 770–778, 2016.
- [5] Ahmet Iscen, Giorgos Tolias, Yannis Avrithis, and Ondrej Chum. Label propagation for deep semi-supervised learning. In *The IEEE Conference on Computer Vision and Pattern Recognition (CVPR)*, page in press, 2019.
- [6] Alex Krizhevsky and Geoffrey Hinton. Learning multiple layers of features from tiny images. Technical report, University of Toronto, 2009.
- [7] Samuli Laine and Timo Aila. Temporal ensembling for semi-supervised learning. In *The International Conference on Learning Representations (ICLR)*, pages 1–13, 2017.
- [8] Yann LeCun, Léon Bottou, Yoshua Bengio, and Patrick Haffner. Gradient-based learning applied to document recognition. *Proceedings of the IEEE*, 86(11):2278–2324, 1998.
- [9] Dong-Hyun Lee. Pseudo-label: The simple and efficient semi-supervised learning method for deep neural networks. In *Workshop on Challenges in Representation Learning, ICML*, volume 3, page 2, 2013.
- [10] Yu Liu, Guanglu Song, Jing Shao, Xiao Jin, and Xiaogang Wang. Transductive centroid projection for semi-supervised large-scale recognition. In *The European Conference on Computer Vision (ECCV)*, volume 11209 of *LNCS*, pages 72–89. Springer, 2018.
- [11] Ilya Loshchilov and Frank Hutter. SGDR: Stochastic gradient descent with warm restarts. *arXiv preprint arXiv:1608.03983*, 2016.
- [12] Takeru Miyato, Shin-ichi Maeda, Shin Ishii, and Masanori Koyama. Virtual adversarial training: a regularization method for supervised and semi-supervised learning. *IEEE Transactions on Pattern Analysis and Machine Intelligence*, page in press, 2018.
- [13] Yuval Netzer, Tao Wang, Adam Coates, Alessandro Bissacco, Bo Wu, and Andrew Y. Ng. Reading digits in natural images with unsupervised feature learning. In *NIPS Workshop on Deep Learning and Unsupervised Feature Learning*, 2011.
- [14] Yunchen Pu, Zhe Gan, Ricardo Henao, Xin Yuan, Chunyuan Li, Andrew Stevens, and Lawrence Carin. Variational autoencoder for deep learning of images, labels and captions. In *Advances in Neural Information Processing Systems 29*, pages 2352–2360, 2016.
- [15] Siyuan Qiao, Wei Shen, Zhishuai Zhang, Bo Wang, and Alan Yuille. Deep co-training for semi-supervised image recognition. In *The European Conference on Computer Vision (ECCV)*, volume 11219 of *LNCS*, pages 142–159. Springer, 2018.
- [16] Thomas Robert, Nicolas Thome, and Matthieu Cord. HybridNet: Classification and reconstruction cooperation for semi-supervised learning. In *The European Conference on Computer Vision (ECCV)*, volume 11211 of *LNCS*, pages 158–175. Springer, 2018.
- [17] Olga Russakovsky, Jia Deng, Hao Su, Jonathan Krause, Sanjeev Satheesh, Sean Ma, Zhiheng Huang, Andrej Karpathy, Aditya Khosla, Michael Bernstein, Alexander C. Berg, and Li Fei-Fei. ImageNet large scale visual recognition challenge. *International Journal of Computer Vision*, 115(3):211–252, 2015.

- [18] Mehdi Sajjadi, Mehran Javanmardi, and Tolga Tasdizen. Regularization with stochastic transformations and perturbations for deep semi-supervised learning. In *Advances in Neural Information Processing Systems 29*, pages 1163–1171, 2016.
- [19] Daiki Tanaka, Daiki Ikami, Toshihiko Yamasaki, and Kiyoharu Aizawa. Joint optimization framework for learning with noisy labels. In *The IEEE Conference on Computer Vision and Pattern Recognition (CVPR)*, pages 5552–5560, 2018.
- [20] Antti Tarvainen and Harri Valpola. Mean teachers are better role models: Weight-averaged consistency targets improve semi-supervised deep learning results. In *Advances in Neural Information Processing Systems 30*, pages 1195–1204, 2017.
- [21] Jason Weston, Frédéric Ratle, Hossein Mobahi, and Ronan Collobert. Deep learning via semi-supervised embedding. In Grégoire Montavon, Geneviève B. Orr, and Klaus-Robert Müller, editors, *Neural Networks: Tricks of the Trade: Second Edition*, pages 639–655. Springer, 2012.
- [22] Kun Yi and Jianxin Wu. Probabilistic end-to-end noise correction for learning with noisy labels. In *The IEEE Conference on Computer Vision and Pattern Recognition (CVPR)*, page in press, 2019.
- [23] Xiaojin Zhu and Zoubin Ghahramani. Learning from labeled and unlabeled data with label propagation. Technical Report CMU-CALD-02-107, Carnegie Mellon University, 2002.

A Proof

A.1 Proof of Theorem 1

Theorem 1 Suppose D2 is trained by SGD with the loss function $\mathcal{L} = \alpha\mathcal{L}_c + \beta\mathcal{L}_e$. Let $\hat{\mathbf{p}}$ denote the prediction by the network for one example and \hat{p}_n is the largest value in $\hat{\mathbf{p}}$. After the optimization algorithm converges, we have $\tilde{p}_n \rightarrow \exp(-\frac{\mathcal{L}}{\alpha}) (\hat{p}_n)^{1-\frac{\beta}{\alpha}}$.

Proof.

First, the loss function can be rewritten by

$$\mathcal{L} = (\alpha - \beta) \sum_{j=1}^N \sigma(\mathbf{W}^\top \mathbf{f})_j \log(\sigma(\mathbf{W}^\top \mathbf{f})_j) - \alpha \sum_{j=1}^N \sigma(\mathbf{W}^\top \mathbf{f})_j \log(\tilde{p}_j). \quad (6)$$

It is easy to see

$$\frac{\partial \sigma(\mathbf{W}^\top \mathbf{f})_j}{\partial \mathbf{w}_n} = \mathbb{I}(j = n) \sigma(\mathbf{W}^\top \mathbf{f})_j \mathbf{f} - \sigma(\mathbf{W}^\top \mathbf{f})_j \sigma(\mathbf{W}^\top \mathbf{f})_n \mathbf{f}. \quad (7)$$

Now we can compute the gradient of \mathcal{L} with respect to \mathbf{w}_n :

$$\begin{aligned} \frac{\partial \mathcal{L}}{\partial \mathbf{w}_n} &= (\alpha - \beta) \sum_{j=1}^N \left[\frac{\partial \sigma(\mathbf{W}^\top \mathbf{f})_j}{\partial \mathbf{w}_n} \log(\sigma(\mathbf{W}^\top \mathbf{f})_j) + \sigma(\mathbf{W}^\top \mathbf{f})_j \frac{\partial \log(\sigma(\mathbf{W}^\top \mathbf{f})_j)}{\partial \mathbf{w}_n} \right] \\ &\quad - \alpha \sum_{j=1}^N \frac{\partial \sigma(\mathbf{W}^\top \mathbf{f})_j}{\partial \mathbf{w}_n} \log(\tilde{p}_j) \end{aligned} \quad (8)$$

$$\begin{aligned} &= (\alpha - \beta) \sum_{j=1}^N \left[\mathbb{I}(j = n) \sigma(\mathbf{W}^\top \mathbf{f})_j \mathbf{f} - \sigma(\mathbf{W}^\top \mathbf{f})_j \sigma(\mathbf{W}^\top \mathbf{f})_n \mathbf{f} \right] \log(\sigma(\mathbf{W}^\top \mathbf{f})_j) \\ &\quad + (\alpha - \beta) \sum_{j=1}^N \sigma(\mathbf{W}^\top \mathbf{f})_j (\mathbb{I}(j = n) \mathbf{f} - \sigma(\mathbf{W}^\top \mathbf{f})_n \mathbf{f}) \\ &\quad - \alpha \sum_{j=1}^N \left[\mathbb{I}(j = n) \sigma(\mathbf{W}^\top \mathbf{f})_j \mathbf{f} - \sigma(\mathbf{W}^\top \mathbf{f})_j \sigma(\mathbf{W}^\top \mathbf{f})_n \mathbf{f} \right] \log(\tilde{p}_j) \end{aligned} \quad (9)$$

$$\begin{aligned} &= (\alpha - \beta) \sigma(\mathbf{W}^\top \mathbf{f})_n \log(\sigma(\mathbf{W}^\top \mathbf{f})_n) \mathbf{f} \\ &\quad - (\alpha - \beta) \sum_{j=1}^N \sigma(\mathbf{W}^\top \mathbf{f})_j \log(\sigma(\mathbf{W}^\top \mathbf{f})_j) \sigma(\mathbf{W}^\top \mathbf{f})_n \mathbf{f} \\ &\quad + (\alpha - \beta) \sigma(\mathbf{W}^\top \mathbf{f})_n \mathbf{f} - (\alpha - \beta) \sigma(\mathbf{W}^\top \mathbf{f})_n \mathbf{f} \sum_{j=1}^N \sigma(\mathbf{W}^\top \mathbf{f})_j \\ &\quad - \alpha \sigma(\mathbf{W}^\top \mathbf{f})_n \log(\tilde{p}_n) \mathbf{f} + \alpha \sum_{j=1}^N \sigma(\mathbf{W}^\top \mathbf{f})_j \log(\tilde{p}_j) \sigma(\mathbf{W}^\top \mathbf{f})_n \mathbf{f} \end{aligned} \quad (10)$$

$$\begin{aligned} &= (\alpha - \beta) \sigma(\mathbf{W}^\top \mathbf{f})_n \log(\sigma(\mathbf{W}^\top \mathbf{f})_n) \mathbf{f} - \alpha \sigma(\mathbf{W}^\top \mathbf{f})_n \log(\tilde{p}_n) \mathbf{f} \\ &\quad - \sigma(\mathbf{W}^\top \mathbf{f})_n \mathbf{f} \left[(\alpha - \beta) \sum_{j=1}^N \sigma(\mathbf{W}^\top \mathbf{f})_j \log(\sigma(\mathbf{W}^\top \mathbf{f})_j) - \alpha \sum_{j=1}^N \sigma(\mathbf{W}^\top \mathbf{f})_j \log(\tilde{p}_j) \right] \\ &\quad + (\alpha - \beta) \sigma(\mathbf{W}^\top \mathbf{f})_n \mathbf{f} - (\alpha - \beta) \sigma(\mathbf{W}^\top \mathbf{f})_n \mathbf{f} \end{aligned} \quad (11)$$

$$= [(\alpha - \beta) \log(\sigma(\mathbf{W}^\top \mathbf{f})_n) - \alpha \log(\tilde{p}_n)] \sigma(\mathbf{W}^\top \mathbf{f})_n \mathbf{f} - \mathcal{L} \sigma(\mathbf{W}^\top \mathbf{f})_n \mathbf{f} \quad (12)$$

$$= [(\alpha - \beta) \log(\sigma(\mathbf{W}^\top \mathbf{f})_n) - \alpha \log(\tilde{p}_n) - \mathcal{L}] \sigma(\mathbf{W}^\top \mathbf{f})_n \mathbf{f} \quad (13)$$

$$= [(\alpha - \beta) \log(\hat{p}_n) - \alpha \log(\tilde{p}_n) - \mathcal{L}] \hat{p}_n \mathbf{f}. \quad (14)$$

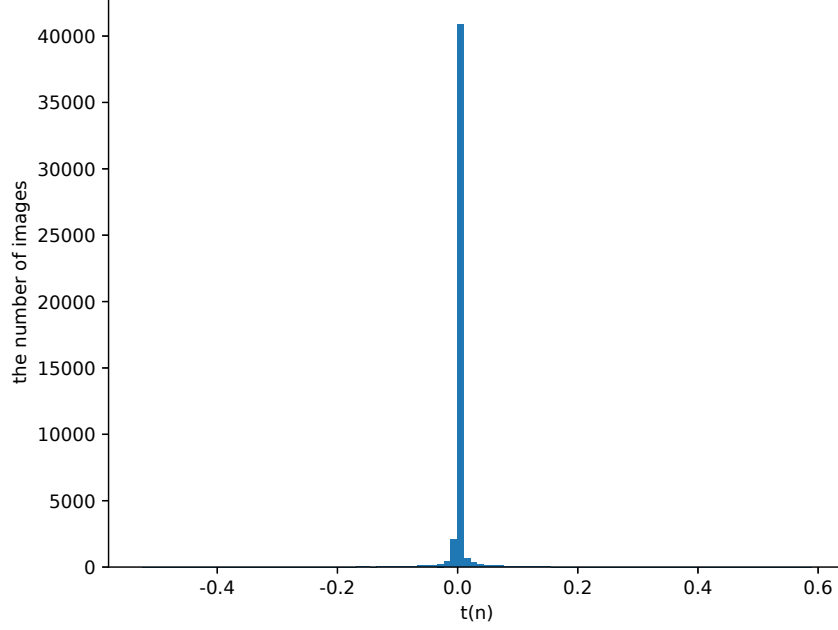


Figure 3: Distribution of $t(n)$ on the whole dataset at the end of the second stage. $t(n)$ is defined as $(\alpha - \beta) \log(\hat{p}_n) - \alpha \log(\tilde{p}_n) - \mathcal{L}$. We can see $t(n) = 0$ for almost all images, where n is calculated according to each image.

During training, we expect the optimization algorithm can converge and finally $\frac{\partial \mathcal{L}}{\partial \mathbf{w}_n} \rightarrow \mathbf{0}$. Because \mathbf{f} can not be $\mathbf{0}$, we conclude that $[(\alpha - \beta) \log(\hat{p}_n) - \alpha \log(\tilde{p}_n) - \mathcal{L}] \hat{p}_n \rightarrow 0$. Because $\sum_{i=1}^N \hat{p}_i = 1$, consider the fact that \hat{p}_n is the largest value in $\{\hat{p}_1, \hat{p}_1, \dots, \hat{p}_N\}$, then $\hat{p}_n \not\rightarrow 0$ at the end of training. So we have $[(\alpha - \beta) \log(\hat{p}_n) - \alpha \log(\tilde{p}_n) - \mathcal{L}] \rightarrow 0$, which states that $\tilde{p}_n \rightarrow \exp(-\frac{\mathcal{L}}{\alpha}) (\hat{p}_n)^{1-\frac{\beta}{\alpha}}$. \square

We would like to show experimental results for verifying this theorem. Let $t(n)$ denote $(\alpha - \beta) \log(\hat{p}_n) - \alpha \log(\tilde{p}_n) - \mathcal{L}$. Now, consider a single sample, suppose $\hat{\mathbf{p}}$ will get the largest value at n where $n \in \{1, 2, \dots, N\}$. Then it is expected that $\hat{p}_n \rightarrow 1$ and $t(n) \rightarrow 0$ at the end of training. Figure 3 shows the distribution of $t(n)$ on the whole dataset, where n is calculated according to different samples. The distribution is almost gathered around 0. So we also observed empirically that $\tilde{p}_n \rightarrow \exp(-\frac{\mathcal{L}}{\alpha}) (\hat{p}_n)^{1-\frac{\beta}{\alpha}}$, where n is the class predicted by the network.

A.2 Proof of Theorem 2

Theorem 2 Suppose $D2$ is trained by SGD with the loss function $\mathcal{L} = \alpha \mathcal{L}_c + \beta \mathcal{L}_e$. If $\tilde{p}_n = \exp(-\frac{\mathcal{L}}{\alpha}) (\hat{p}_n)^{1-\frac{\beta}{\alpha}}$, we must have $\tilde{p}_n \leq \hat{p}_n$.

Proof.

First, according to the loss function we defined, we have

$$\mathcal{L} = \alpha \sum_{j=1}^N \hat{p}_j [\log(\hat{p}_j) - \log(\tilde{p}_j)] - \beta \sum_{j=1}^N \hat{p}_j \log(\hat{p}_j) \quad (15)$$

$$\geq -\beta \sum_{j=1}^N \hat{p}_j \log(\hat{p}_j) \quad (16)$$

$$\geq -\beta \sum_{j=1}^N \hat{p}_j \log(\hat{p}_n) \quad (17)$$

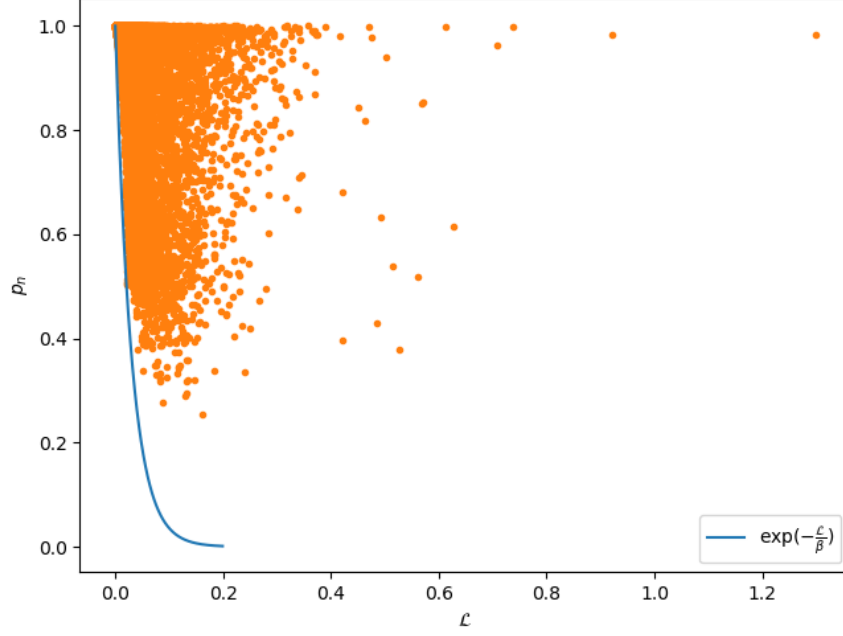


Figure 4: The curve of $\exp(-\frac{\mathcal{L}}{\beta})$ and (\mathcal{L}, p_n) at the end of the second stage.

$$= -\beta \log(\hat{p}_n), \quad (18)$$

where \hat{p}_n is the largest value in $\{\hat{p}_1, \hat{p}_2, \dots, \hat{p}_N\}$. Then, from $\tilde{p}_n = \exp(-\frac{\mathcal{L}}{\alpha}) \hat{p}_n^{1-\frac{\beta}{\alpha}}$ and $\mathcal{L} \geq -\beta \log(\hat{p}_n)$, we have

$$\tilde{p}_n = \exp\left(-\frac{\mathcal{L}}{\alpha}\right) \hat{p}_n^{1-\frac{\beta}{\alpha}} \leq \exp\left(\frac{\beta \log(\hat{p}_n)}{\alpha}\right) \hat{p}_n^{1-\frac{\beta}{\alpha}} = \hat{p}_n. \quad (19)$$

□

Next, we show that $\tilde{p}_n \leq \hat{p}_n$ holds in experiments. With $\tilde{p}_n = \exp(-\frac{\mathcal{L}}{\alpha}) \hat{p}_n^{1-\frac{\beta}{\alpha}}$, if $\tilde{p}_n \leq \hat{p}_n$, that yields $\exp(-\frac{\mathcal{L}}{\alpha}) \hat{p}_n^{1-\frac{\beta}{\alpha}} \leq \hat{p}_n$. Then we can get $\hat{p}_n \geq \exp(-\frac{\mathcal{L}}{\beta})$. Figure 4 shows \hat{p}_n versus $\exp(-\frac{\mathcal{L}}{\beta})$, in which $\beta = 0.03$. For a specific loss value, if p_n is above the function curve, \tilde{p}_n is smaller than p_n . Figure 4 shows the scatter plot of (\mathcal{L}, \hat{p}_n) at the end of the second stage. Almost all points are above the curve. That means if $\tilde{p}_n \rightarrow \exp(-\frac{\mathcal{L}}{\alpha}) \hat{p}_n^{1-\frac{\beta}{\alpha}}$, \tilde{p}_n will be smaller than \hat{p}_n .

A.3 The complete derivation of $\frac{\partial \mathcal{L}}{\partial \tilde{y}_n}$

\mathcal{L} is defined as $\mathcal{L} = \alpha \sum_{j=1}^N \hat{p}_j [\log(\hat{p}_j) - \log(\tilde{p}_j)] - \beta \sum_{j=1}^N \hat{p}_j \log(\hat{p}_j)$, in which $\hat{\mathbf{p}} = \sigma(\hat{\mathbf{y}})$ and $\tilde{\mathbf{p}} = \sigma(\tilde{\mathbf{y}})$. The gradient of \mathcal{L} with respect to \tilde{y}_n is

$$\frac{\partial \mathcal{L}}{\partial \tilde{y}_n} = \sum_{k=1}^N \frac{\partial \mathcal{L}}{\partial \tilde{p}_k} \frac{\partial \tilde{p}_k}{\partial \tilde{y}_n} \quad (20)$$

$$= -\alpha \sum_{k=1}^N \sigma(\hat{\mathbf{y}})_k \frac{1}{\tilde{p}_k} (\mathbb{I}(k=n) \sigma(\tilde{\mathbf{y}})_k - \sigma(\tilde{\mathbf{y}})_k \sigma(\tilde{\mathbf{y}})_n) \quad (21)$$

$$= -\alpha \sum_{k=1}^N \sigma(\hat{\mathbf{y}})_k \frac{1}{\sigma(\tilde{\mathbf{y}})_k} (\mathbb{I}(k=n) \sigma(\tilde{\mathbf{y}})_k - \sigma(\tilde{\mathbf{y}})_k \sigma(\tilde{\mathbf{y}})_n) \quad (22)$$

$$= -\alpha \sum_{k=1}^N \sigma(\hat{\mathbf{y}})_k (\mathbb{I}(k=n) - \sigma(\tilde{\mathbf{y}})_n) \quad (23)$$

$$= -\alpha \sum_{k=1}^N \sigma(\hat{\mathbf{y}})_k \mathbb{I}(k = n) + \alpha \sum_{k=1}^N \sigma(\hat{\mathbf{y}})_k \sigma(\tilde{\mathbf{y}})_n \quad (24)$$

$$= -\alpha \sigma(\hat{\mathbf{y}})_n + \alpha \sigma(\tilde{\mathbf{y}})_n \sum_{k=1}^N \sigma(\hat{\mathbf{y}})_k \quad (25)$$

$$= -\alpha \sigma(\hat{\mathbf{y}})_n + \alpha \sigma(\tilde{\mathbf{y}})_n . \quad (26)$$

B More implementation details

Note that we trained the network using stochastic gradient descent with Nesterov momentum 0.9 in all experiments. We set $\alpha = 0.1$, $\beta = 0.03$ and $\lambda = 4000$ on *all* datasets, which shows the robustness of our method to these hyperparameters. Other hyperparameters (e.g., batch size, learning rate, and weight decay) were set according different datasets.

B.1 ImageNet

Following the prior work [15, 18, 14, 20], we uniformly choose 10% data from training images as labeled data. That means there are 128 labeled data for each category. The rest of training images are considered as unlabeled data. We test our model on the validation set. The backbone network was ResNet-18 [4]. The data augmentation we used is the same as that of [20], which includes random rotation, random resized crop to 224×224 , random horizontal flip and color jittering.

In the first stage, we trained ResNet-18 [4] on 4 GPUs with the labeled data. We trained for 60 epochs with the weight decay of 5×10^{-5} . Because the labeled dataset only contains 128000 images, the batch size was set as 160 to make the parameters update more times. The learning rate was 0.1 at the beginning and decreased by cosine annealing [11] so that it would reach 0 after 75 epochs.

In the second stage, we trained for 60 epochs on 4 GPUs. We set the batch size as 800, 200 of which were labeled. The learning rate was 0.12 and did not change in this stage. During this stage, we found that pseudo-labels would be more accurate. Note that the capacity of ResNet-18 is small and it is hard for ResNet-18 to remember all pseudo-labels. To make pseudo-labels more accurate when repredicting, we finetuned the model using the dataset with pseudo-label. We finetuned for 60 epochs with initial learning rate 0.12 and decayed it with cosine annealing [11] so that it would reach 0 after 65 epochs.

Repeating the second stage, we used the network at the end of last stage to repredict the pseudo-labels of unlabeled images. Then we trained the network and optimize pseudo-labels for 30 epochs with learning rate 0.04. Other settings were the same as the second stage.

In the third stage, we used the pseudo-labels at the end of last stage to finetune the model. We finetuned for 60 epochs with initial learning rate 0.04 and decayed it with cosine annealing [11] so that it would reach 0 after 65 epochs.

B.2 CIFAR-10

Following [7, 12, 20, 15, 16], we used 4000 images (400 per class) from 50000 training images as labeled data and the rest images as unlabeled data. We report the error rates on the full 10000 testing images. The backbone network was Shake-Shake [3]. The data augmentation contained random translations, random horizontal flip and cutout [1].

In the first stage, we trained the Shake-Shake network on 1 GPU with 4000 labeled images. To make the parameters update more times, we set the batch size as 40 and trained the network for 300 epochs. So the parameters of the network could update 100 times per epoch and update 30000 times totally in this stage. The initial learning rate was 0.05 and decreased by cosine annealing [11] so that it would reach 0 after 350 epochs. The weight decay was set as 0.0002.

In the second stage, we optimized the network and pseudo-labels for 300 epochs on 4 GPUs. The batch size was 512, in which 128 images were labeled and others were unlabeled. The learning rate was 0.12 and did not change in this stage.

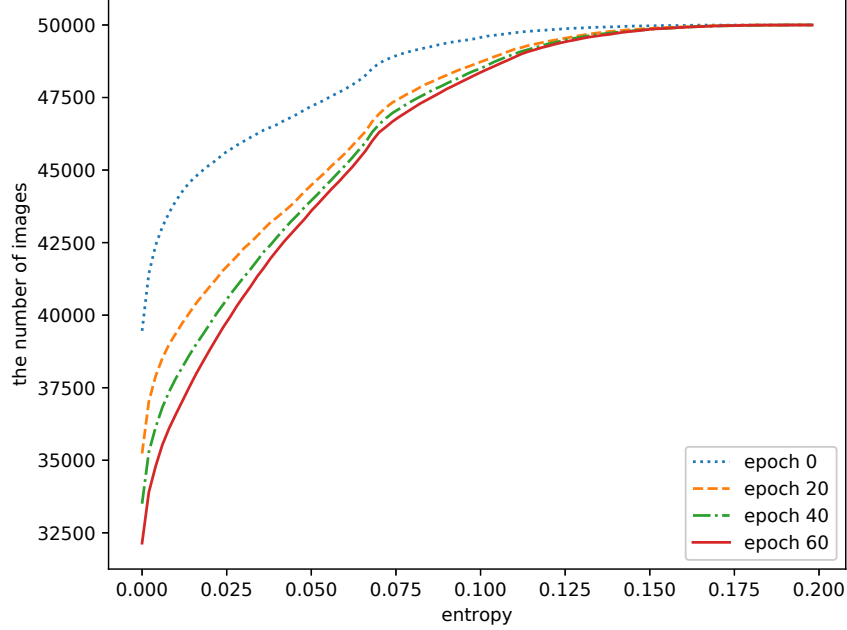


Figure 5: Cumulative distribution of the number of pseudo-labels versus the entropy. For each point (n, e) on the line, it means there are n images whose label entropies are less than e . Pseudo-labels will become flat as the D2 framework is trained more epochs.

Repeating the second stage, we repredicted pseudo-labels at 0, 75, 150, 225 epoch. After each reprediction, we optimized the network and pseudo-labels for 75 epochs. The learning rate were set as 0.12, 0.08, 0.04, 0.004, respectively. Other settings were the same as the second stage.

In the third stage, we finetuned the network for 50 epochs with batch size 512. The learning rate was 0.01 at the beginning and decreased by cosine annealing [11] so that it would reach 0 at the end.

B.3 SVHN

Following [7, 20, 12, 15], we use 1000 images (100 per class) as labeled data and the rest 72257 training images as unlabeled data. The backbone network was ConvLarge [7]. The data augmentation consists of adding gaussian noise to images like [7, 20] and cutout [1].

The settings of learning rates and weight decay were the same as that of our training strategy for CIFAR-10. In the first stage, we trained the ConvLarge [7] network on 1 GPU for 180 epochs with batch size 10. In the second stage, the batch size was set as 512, in which 128 images were labeled. The network was trained for 180 epochs. Repeating the second stage, pseudo-labels were repredicted at 0, 45, 90, 135 epoch. In the third stage, we finetuned the network for 180 epochs.

C Additional figures

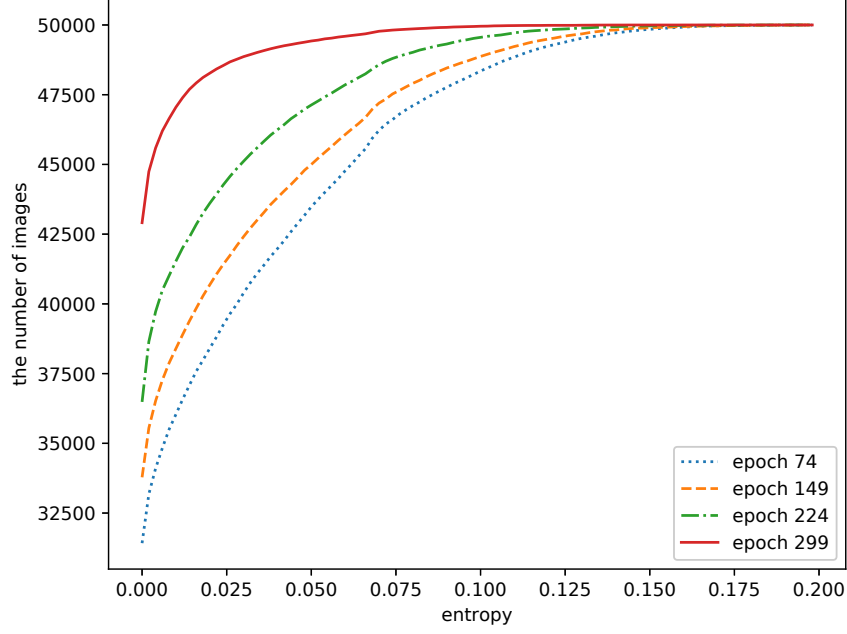


Figure 6: Cumulative distribution of the number of pseudo-labels versus the entropy after using the repetitive prediction (R2) strategy. For each point (n, e) on the line, it means there are n images whose label entropies are less than e . Using the R2 strategy can make pseudo-labels more sharp at the end of training.

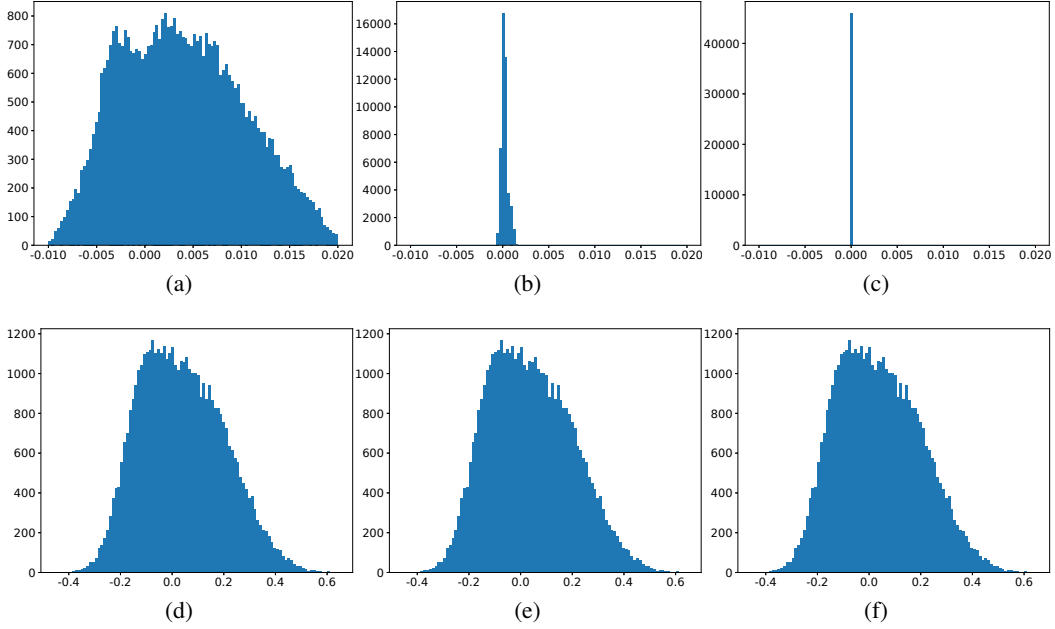


Figure 7: During the second stage, the distributions of $\sum_{i=1}^N \hat{y}_i$ on the unlabeled samples at 100, 200, 300 epoch are showed by (a), (b), (c), respectively. Note that $\sum_{i=1}^N \hat{y}_i$ will get more and more concentrated with training. The distributions of $\sum_{i=1}^N \tilde{y}_i$ on the unlabeled samples at 100, 200, 300 epoch are showed by (d), (e), (f), respectively. According to our analysis, $\sum_{i=1}^N \tilde{y}_i$ will not change. Experimental results are consistent with our theoretical analysis.

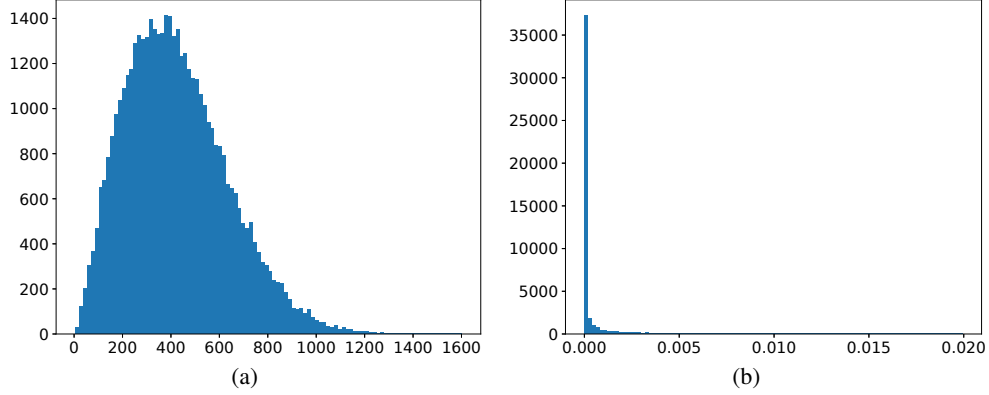


Figure 8: (a) shows the distributions of the number of images versus $\|\tilde{\mathbf{y}}\|_2$. (b) shows the distributions of the number of images versus $\|\frac{\partial \mathcal{L}}{\partial \tilde{\mathbf{y}}}\|_2$. Note that the ranges of x-axis are *different* between (a) and (b). From the figure, we can see $\frac{\partial \mathcal{L}}{\partial \tilde{\mathbf{y}}} = -\alpha \sigma(\hat{\mathbf{y}}) + \alpha \sigma(\tilde{\mathbf{y}})$ is far less than $\tilde{\mathbf{y}}$. So we use one more hyperparameter λ rather than the overall learning rate to update the pseudo logit $\tilde{\mathbf{y}}$.

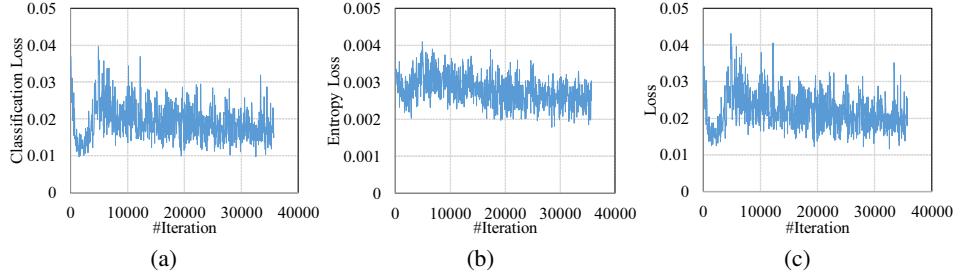


Figure 9: (a), (b), (c) show how \mathcal{L}_c , \mathcal{L}_e , \mathcal{L} change by training D2 without R2 (line a in Table 1), respectively. With a fixed learning rate, it is difficult for these loss terms to decrease.

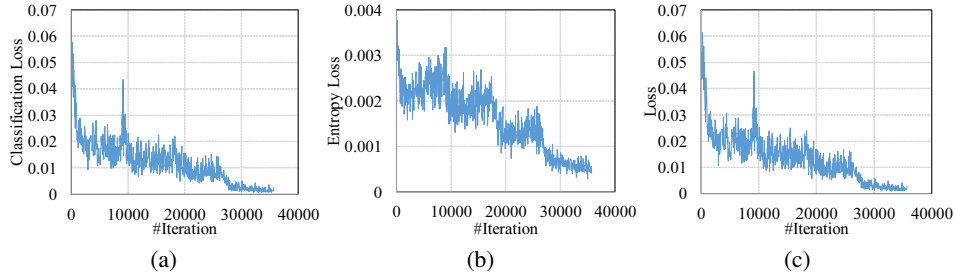


Figure 10: (a), (b), (c) show how \mathcal{L}_c , \mathcal{L}_e , \mathcal{L} change by training D2 with R2 (line e in Table 1), respectively. Reprediction occurs at 0, 8750, 17500, and 26250 iterations. After each reprediction, we decrease the learning rate.

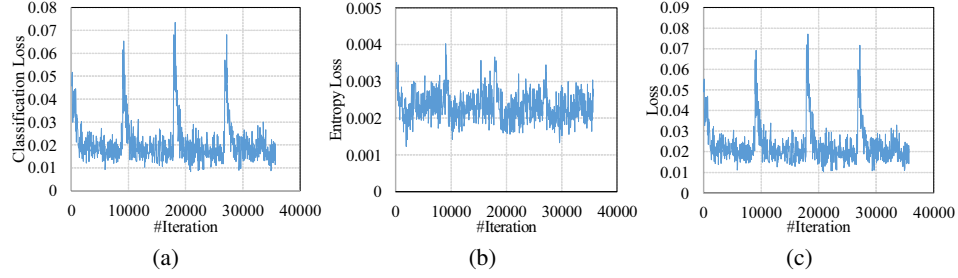


Figure 11: (a), (b), (c) show how \mathcal{L}_c , \mathcal{L}_e , \mathcal{L} change by training D2 with only reprediction (line c in Table 1), respectively. Reprediction occurs at 0, 8750, 17500, and 26250 iterations. Without reducing the learning rate, the loss can not decrease and network prediction keep flat. So pseudo-labels will not become sharp.

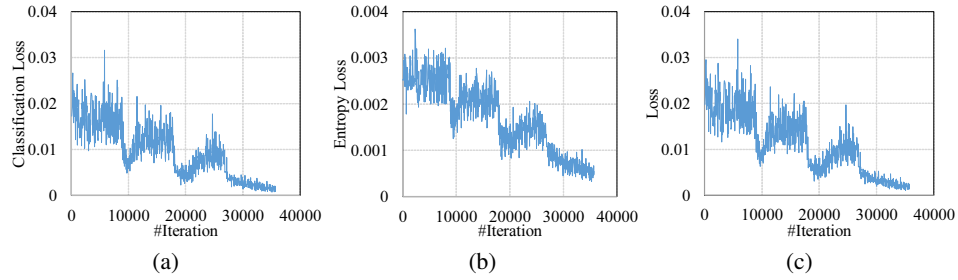


Figure 12: (a), (b), (c) show how \mathcal{L}_c , \mathcal{L}_e , \mathcal{L} change by training D2 with only reducing learning rate (line d in Table 1), respectively. Reducing learning rate occurs at 8750, 17500, and 26250 iterations. It can make loss decrease. But the learning algorithm is still impacted by the equality condition bias.